Applied Numerical Mathematics ••• (••••) •••–•••

Contents lists available at ScienceDirect

Applied Numerical Mathematics

www.elsevier.com/locate/apnum

Fokas transform method for a brain tumor invasion model with heterogeneous diffusion in $1+1$ dimensions ☆

D. Mantzavinos [a], M.G. Papadomanolaki [b], Y.G. Saridakis [b,*], A.G. Sifalakis [b]

[a] *Department of Applied Mathematics and Theorical Physics, University of Cambridge, Cambridge CB3 0WA, UK*
[b] *Applied Mathematics & Computers Lab, Department of Sciences, Technical University of Crete, Chania 73100, Greece*

ARTICLE INFO

Article history:
Available online xxxx

Keywords:
Gliomas
Discontinuous diffusion coefficient
Fokas approach
Fourier transform

ABSTRACT

Gliomas are among the most aggressive forms of brain tumors. Over the last years mathematical models have been well developed to study gliomas growth. We consider a simple and well established mathematical model focused on proliferation and diffusion. Due to the heterogeneity of the brain tissue (white and grey matter) the diffusion coefficient is considered to be discontinuous. Fokas transform approach for the solution of linear PDE problems, apart from the fact that it avoids solving intermediate ODE problems, yields novel integral representations of the solution in the complex plane that decay exponentially fast and converge uniformly at the boundaries. To take advantage of these properties for the solution of the model problem at hand, we have successfully implemented Fokas transform method in the multi-domain environment induced by the interface discontinuities of our problem's domain. The fact that the integral representation of the solution at any time–space point of our problem's domain is independent on any other points of the domain, except of course on initial data, coupled with a simple composite trapezoidal rule, implemented on appropriately chosen integration contours, yields a fast and efficient analytical–numerical technique capable of producing directly high-order approximations of the solution at any point of the domain requiring no prior knowledge of the solution at any other time instances or space information.

1. Introduction

Gliomas, the most common primary brain tumors, are well known to be highly invasive. Recent mathematical models [7,1,2,15,18] formulated the problem of glioma growth where the basic parameters of the models were estimated by CT scan data. These models focus on two parameters: the spread D of glioma cells to tissues and the net proliferation rate ρ of glioma cells. Swanson [11,13,14,12] developed a model based on the differential motility of gliomas cells in white and grey matter suggesting that the diffusion coefficient in white matter is greater than in grey matter. Key role in the mathematical formulation of the problem plays the differential equation:

$$\frac{\partial \bar{c}}{\partial \bar{t}} = \nabla \cdot \left(\bar{D}(\bar{\mathbf{x}})\nabla \bar{c}\right) + \rho \bar{c}, \tag{1}$$

☆ This work was supported by ESF/GR-NSRF-THALIS under the contract number MIS 379416.
* Corresponding author.
E-mail address: yiannis@science.tuc.gr (Y.G. Saridakis).

http://dx.doi.org/10.1016/j.apnum.2014.09.006
0168-9274/

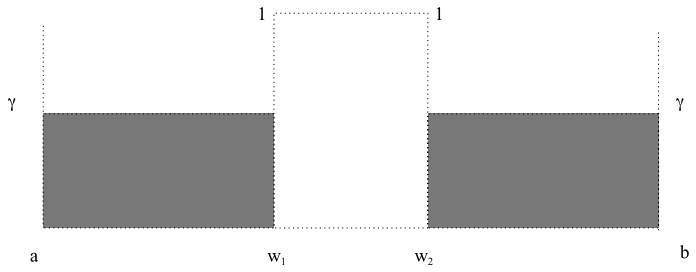

Fig. 1. Diffusion coefficient.

where $\bar{c}(\bar{\mathbf{x}},\bar{t})$ denotes the tumor cell density at location $\bar{x}$ and time $\bar{t}$, ρ denotes the net proliferation rate, and $\bar{D}(\bar{\mathbf{x}})$ is the diffusion coefficient representing the active motility of malignant cells satisfying

$$\bar{D}(\bar{\mathbf{x}}) = \begin{cases} D_g, & \bar{\mathbf{x}} \text{ in grey matter} \\ D_w, & \bar{\mathbf{x}} \text{ in white matter} \end{cases}, \tag{2}$$

with D_g and D_w scalars and $D_w > D_g$. The model formulation is completed by zero flux boundary conditions which impose no migration of cells beyond the brain boundaries and an initial condition $\bar{c}(\bar{\mathbf{x}},0) = \bar{f}(\bar{\mathbf{x}})$, where $\bar{f}(\bar{x})$ is the initial spatial distribution of malignant cells.

In this work, we consider the dimensionless form of the previous model in one dimension and on a finite domain (grey matter – white matter – grey matter). By making use [11] the dimensionless variables:

$$x = \sqrt{\frac{\rho}{D_w}}\bar{x}, \tag{3}$$

$$t = \rho\bar{t}, \tag{4}$$

$$c(x,t) = \bar{c}\left(\sqrt{\frac{\rho}{D_w}}\bar{x}\rho\bar{t}\right)\frac{D_w}{\rho N_0}, \tag{5}$$

$$f(x) = \bar{f}\left(\sqrt{\frac{\rho}{D_w}}\bar{x}\right) \tag{6}$$

with $N_0 = \int \bar{f}(\bar{x})d\bar{x}$ to denote the initial number of tumor cells in the brain at $\bar{t} = 0$, we arrive at the dimensionless system:

$$\begin{cases} c_t = (Dc_x)_x + c, & x \in [a,b],\ t \geq 0 \\ c_x(a,t) = 0 \quad \text{and} \quad c_x(b,t) = 0 \\ c(x,0) = f(x) \end{cases} \tag{7}$$

and by substituting

$$c(x,t) = e^t u(x,t) \tag{8}$$

we obtain

$$\begin{cases} u_t = (Du_x)_x, & x \in [a,b],\ t \geq 0 \\ u_x(a,t) = 0 \quad \text{and} \quad u_x(b,t) = 0\,. \\ u(x,0) = f(x) \end{cases} \tag{9}$$

Note that the initial source of tumor cells $f(x)$ is defined through out of this paper to be:

$$f(x) := \delta(x-\xi), \quad \xi \in (a,b) \tag{10}$$

where $\delta(x)$ denotes the Dirac's delta function. Furthermore, the dimensionless parameter D is considered to be constant defined by:

$$D(x) = \begin{cases} \gamma, & a \leq x < w_1 \\ 1, & w_1 \leq x < w_2 \\ \gamma, & w_2 \leq x \leq b \end{cases}, \tag{11}$$

where $\gamma := D_g/D_w < 1$ is the dimensionless diffusion coefficient in grey matter and the dimensionless diffusion coefficient in white matter is to considered to be unity (see Fig. 1). Estimates of the values of the physiological parameters for a high grade tumor are included in Table 1 (cf. [11] and the references therein).

Please cite this article in press as: D. Mantzavinos et al., Fokas transform method for a brain tumor invasion model with heterogeneous diffusion in $1+1$ dimensions, Applied Numerical Mathematics (2014), http://dx.doi.org/10.1016/j.apnum.2014.09.006

Table 1
Parameter estimates for a high-grade human glioma.

Parameter	Symbol	Range of values	Units
Diffusion coefficient in grey matter	D_g	0.0013	cm^2/day
Diffusion coefficient in white matter	D_w	$> 4D_g = 0.0052$	cm^2/day
Net growth rate	ρ	0.012	day^{-1}

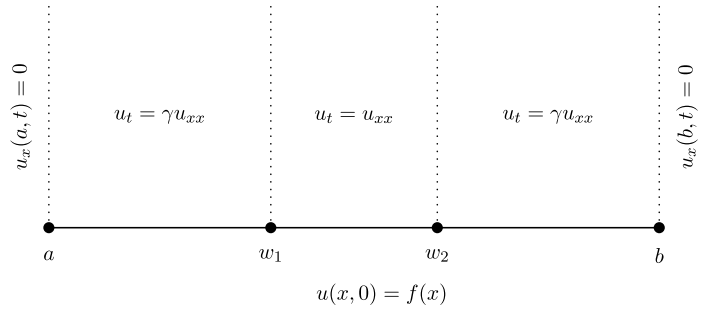

Fig. 2. Model problem.

Observe now that the discontinuous diffusion coefficient $D(x)$ directly implies discontinuity of u_x, hence continuity of Du_x, across each interface. In fact, as the linear parabolic nature of the initial-boundary value problem (9) implies continuity u across each interface, that is

$$[u] := u^+ - u^- = 0, \quad \text{at } x = w_k,\ k = 1, 2, \tag{12}$$

where

$$u^+ := \lim_{x \to w_k^+} u(x) \quad \text{and} \quad u^- := \lim_{x \to w_k^-} u(x),$$

integration of the equation in (9) over the discontinuity interfaces yields

$$[Du_x] := D^+ u_x^+ - D^- u_x^- = 0, \quad \text{at } x = w_k,\ k = 1, 2. \tag{13}$$

By using the above continuity constrains (12)–(13) we can alternatively describe the model problem in (9) by

$$\begin{cases} u_t = Du_{xx}, \quad x \in \mathcal{R}_\ell,\ \ell = 1, 2, 3,\ t \geq 0 \\ u_x(a,t) = 0 \quad \text{and} \quad u_x(b,t) = 0 \\ [u] = 0 \quad \text{and} \quad [Du_x] = 0 \quad \text{at } x = w_k,\ k = 1, 2 \\ u(x,0) = f(x) \end{cases} \tag{14}$$

where $\mathcal{R}_\ell$ denote the region

$$\mathcal{R}_1 := [a, w_1], \qquad \mathcal{R}_2 := [w_1, w_2], \qquad \mathcal{R}_3 := [w_2, b]. \tag{15}$$

The above definition of the model problem is graphically depicted in Fig. 2.

Triggered by the application's significance as well as the presence of interface discontinuities, we initiated an investigation pertaining to the efficient implementation of the Fokas transform method in the above described multi-domain environment. Fokas method [4,5] combines complex analysis with numerics to construct a novel technique for numerically evaluating the integral representation of the solution of the partial differential equation. The recent works of Flyer and Fokas [3] (see also [6]) and Papatheodorou and Kandili [9] dealt with the problem of implementing Fokas method for the heat equation with Dirichlet boundary conditions. It was shown that, as the method allows the solution to be computed at any point of the time–space domain without requiring any knowledge of the solution at any other point of the domain, it has a significant advantage over the classical numerical techniques especially when remote time calculations are needed. The efficient implementation of Fokas method in the present work preserves this advantage for the multi-domain case as well.

The work in this paper is organized as follows: In Section 2 we appropriately extend Fokas method for the multi-domain problem at hand and present the integral form of the solution in each domain. For the efficient numerical evaluation of the integrals involved we use, in Section 3, the integrand analyticity properties to properly deform the integration contours while, in Section 4, we reveal integrand inherent symmetry properties.

Please cite this article in press as: D. Mantzavinos et al., Fokas transform method for a brain tumor invasion model with heterogeneous diffusion in $1+1$ dimensions, Applied Numerical Mathematics (2014), http://dx.doi.org/10.1016/j.apnum.2014.09.006

2. Fokas integral representation of the solution

Let $u_\ell(x,t)$, $\ell = 1,2,3$ denote the solution of the model problem (14) in the $\mathcal{R}_\ell$, $\ell = 1,2,3$ region respectively. Apparently then, the constrains in (12)–(13) are equivalently written as:

$$u_1(w_1,t) = u_2(w_1,t) \tag{16}$$

$$\gamma u_{1x}(w_1,t) = u_{2x}(w_1,t) \tag{17}$$

$$u_2(w_2,t) = u_3(w_2,t) \tag{18}$$

$$u_{2x}(w_2,t) = \gamma u_{3x}(w_2,t) \tag{19}$$

Fokas transform method uses the *divergent form* of the differential equation to produce the so called *Global Relation* which is used in the sequel to derive the integral form of the solution. A detailed description of the steps involved in the derivation of the solution's integral form may be found in [5]. Here, we will briefly describe the procedure, aiming in emphasizing the unknown quantities involved due to the usage of compatibility, rather than boundary, conditions at the interior interface points. In this direction, observe that $u_1(x,t)$ satisfies equation

$$u_{1t} = \gamma u_{1xx}, \quad x \in \mathcal{R}_1 \tag{20}$$

or, equivalently, in *divergence form*, equation

$$\left[e^{-ikx+\gamma k^2 t}u_1\right]_t - \left[e^{-ikx+\gamma k^2 t}\gamma(u_{1x} + i\kappa u_1)\right]_x = 0, \quad k \in \mathbb{C}. \tag{21}$$

Integrating over space and time, and applying Green's theorem one obtains that

$$\begin{aligned}
&\int_a^{w_1} e^{-ikx+\gamma k^2 t}u_1(x,t)dx - \int_a^{w_1} e^{-ikx}u_1(x,0)dx \\
&\quad - \int_0^t \gamma e^{-ikw_1+\gamma k^2\tau}u_{1x}(w_1,\tau)d\tau - \int_0^t ik\gamma e^{-ikw_1+\gamma k^2\tau}u_1(w_1,\tau)d\tau \\
&\quad + \int_0^t \gamma e^{-ika+\gamma k^2\tau}u_{1x}(a,\tau)d\tau + \int_0^t ik\gamma e^{-ika+\gamma k^2\tau}u_1(a,\tau)d\tau = 0
\end{aligned} \tag{22}$$

to observe that, besides $u_1(x,t)$, quantities $u_1(w_1,\tau)$ and $u_{1x}(w_1,\tau)$ are also unknown. Let us now denote the direct Fourier transform of $u_\ell(x,t)$ by

$$\widehat{u}_\ell(k,t) = \int_{l_\ell}^{r_\ell} e^{-ikx}u_\ell(x,t)dx, \quad k \in \mathbb{C},\ \ell = 1,2,3 \tag{23}$$

and the inverse Fourier transform by

$$u_\ell(x,t) = \frac{1}{2\pi}\int_{-\infty}^{\infty} e^{ikx}\widehat{u}_\ell(k,t)dk, \quad \ell = 1,2,3 \tag{24}$$

where l_ℓ and r_ℓ denote the left and right endpoints of the $\mathcal{R}_\ell$ region. If we also define

$$\widetilde{u}_\ell\left(x,\gamma k^2\right) := \int_0^t e^{\gamma k^2\tau}u_\ell(x,\tau)d\tau, \quad \ell = 1,3 \tag{25}$$

$$\widetilde{u}_2\left(x,k^2\right) := \int_0^t e^{k^2\tau}u_2(x,\tau)d\tau \tag{26}$$

and

Please cite this article in press as: D. Mantzavinos et al., Fokas transform method for a brain tumor invasion model with heterogeneous diffusion in $1+1$ dimensions, Applied Numerical Mathematics (2014), http://dx.doi.org/10.1016/j.apnum.2014.09.006

$$\widetilde{u}_{\ell x}(x,\gamma k^2) := \int_0^t e^{\gamma k^2 \tau} u_{\ell x}(x,\tau)\,d\tau, \quad \ell = 1,3 \tag{27}$$

$$\widetilde{u}_{2x}(x,k^2) := \int_0^t e^{k^2 \tau} u_{2x}(x,\tau)\,d\tau \tag{28}$$

then Eq. (22) becomes the *Global Relation* of region $\mathcal{R}_1$:

$$\begin{aligned} e^{\gamma k^2 t}\widehat{u}_1(k,t) = \widehat{f}_1(k) &+ \gamma e^{-ikw_1}\left[\widetilde{u}_{1x}(w_1,\gamma k^2) + ik\widetilde{u}_1(w_1,\gamma k^2)\right] \\ &- \gamma e^{-ika}\left[\widetilde{u}_{1x}(a,\gamma k^2) + ik\widetilde{u}_1(a,\gamma k^2)\right], \quad k \in \mathbb{C} \end{aligned} \tag{29}$$

where:

$$\widehat{f}_\ell(r) = \int_{l_\ell}^{r_\ell} e^{-irx} f_\ell(x)\,dx \tag{30}$$

with f_ℓ denoting the initial condition $u(x,0)$ in $\mathcal{R}_\ell$, $\ell = 1,2,3$. Working similarly, the Global relations for regions $\mathcal{R}_2$ and $\mathcal{R}_3$ are given respectively by

$$\begin{aligned} e^{k^2 t}\widehat{u}_2(k,t) = \widehat{f}_2(k) &+ e^{-ikw_2}\left[\widetilde{u}_{2x}(w_2,k^2) + ik\widetilde{u}_2(w_2,k^2)\right] \\ &- e^{-ikw_1}\left[\widetilde{u}_{2x}(w_1,k^2) + ik\widetilde{u}_2(w_1,k^2)\right], \quad k \in \mathbb{C} \end{aligned} \tag{31}$$

and

$$\begin{aligned} e^{\gamma k^2 t}\widehat{u}_3(k,t) = \widehat{f}_3(k) &+ \gamma e^{-ikb}\left[\widetilde{u}_{3x}(b,\gamma k^2) + ik\widetilde{u}_3(b,\gamma k^2)\right] \\ &- \gamma e^{-ikw_2}\left[\widetilde{u}_{3x}(w_2,\gamma k^2) + ik\widetilde{u}_3(w_2,\gamma k^2)\right], \quad k \in \mathbb{C}. \end{aligned} \tag{32}$$

Moreover, taking into consideration constrains (16)–(19), the boundary conditions $u_x(a,t) = 0$ and $u_x(b,t) = 0$, and if we let $\lambda^2 = \gamma k^2$ and $c = \gamma^{-\frac{1}{2}}$, and relabel in the sequel λ to k, the above relations take the form:

$$\begin{aligned} e^{k^2 t}\widehat{u}_1(ck,t) = \widehat{f}_1(ck) &+ \gamma e^{-ickw_1}\left[\widetilde{u}_{1x}(w_1,k^2) + ick\widetilde{u}_1(w_1,k^2)\right] \\ &- \gamma e^{-icka} ick\widetilde{u}_1(a,k^2), \quad k \in \mathbb{C} \end{aligned} \tag{33}$$

$$\begin{aligned} e^{k^2 t}\widehat{u}_2(k,t) = \widehat{f}_2(k) &+ e^{-ikw_2}\left[\widetilde{u}_{2x}(w_2,k^2) + ik\widetilde{u}_2(w_2,k^2)\right] \\ &- e^{-ikw_1}\left[\gamma\widetilde{u}_{1x}(w_1,k^2) + ik\widetilde{u}_1(w_1,k^2)\right], \quad k \in \mathbb{C} \end{aligned} \tag{34}$$

$$\begin{aligned} e^{k^2 t}\widehat{u}_3(ck,t) = \widehat{f}_3(ck) &+ \gamma e^{-ickb} ick\widetilde{u}_3(b,k^2) \\ &- \gamma e^{-ickw_2}\left[\frac{1}{\gamma}\widetilde{u}_{2x}(w_2,k^2) + ick\widetilde{u}_2(w_2,k^2)\right], \quad k \in \mathbb{C}. \end{aligned} \tag{35}$$

Inverting the Fourier transforms in Eqs. (33)–(35) we obtain the integral representation of the solutions $u_\ell(x,t)$, $\ell = 1,2,3$ respectively:

$$u_1(x,t) = \frac{c}{2\pi}\int_{-\infty}^{\infty} e^{ickx} e^{-k^2 t}\widehat{f}_1(ck)\,dk \tag{36a}$$

$$- \frac{1}{2c\pi}\int_{-\infty}^{\infty} e^{ick(x-w_1)} e^{-k^2 t}\left[\widetilde{u}_{1x}(w_1,k^2) + ick\widetilde{u}_1(w_1,k^2)\right]dk \tag{36b}$$

$$- \frac{1}{2\pi}\int_{-\infty}^{\infty} ike^{ick(x-a)} e^{-k^2 t}\widetilde{u}_1(a,k^2)\,dk \tag{36c}$$

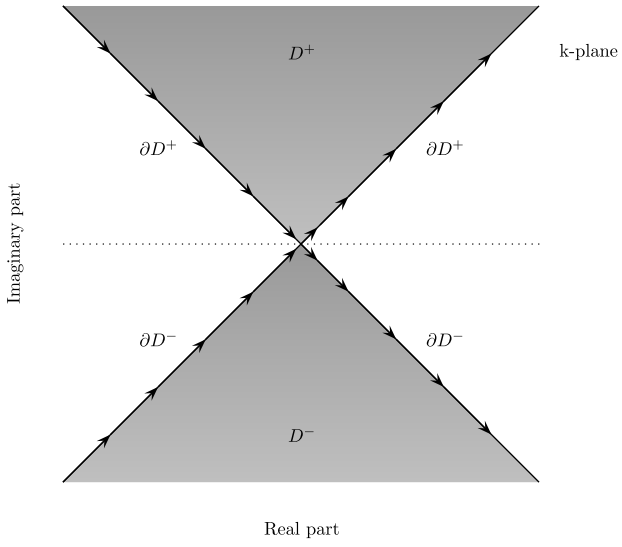

Fig. 3. The contours ∂D^+ and ∂D^-.

$$u_2(x,t) = \frac{1}{2\pi}\int_{-\infty}^{\infty} e^{ikx-k^2t}\hat{f}_2(k)dk \tag{37a}$$

$$-\frac{1}{2\pi}\int_{-\infty}^{\infty} e^{ik(x-w_2)}e^{-k^2t}\left[\tilde{u}_{2x}(w_2,k^2)+ik\tilde{u}_2(w_2,k^2)\right]dk \tag{37b}$$

$$-\frac{1}{2\pi}\int_{-\infty}^{\infty} e^{ik(x-w_1)}e^{-k^2t}\left[\gamma\tilde{u}_{1x}(w_1,k^2)+ik\tilde{u}_1(w_1,k^2)\right]dk \tag{37c}$$

$$u_3(x,t) = \frac{c}{2\pi}\int_{-\infty}^{\infty} e^{ickx-k^2t}\hat{f}_3(ck)dk \tag{38a}$$

$$-\frac{1}{2\pi}\int_{-\infty}^{\infty} e^{ick(x-b)}e^{-k^2t}ik\tilde{u}_3(b,k^2)dk \tag{38b}$$

$$-\frac{1}{2c\pi}\int_{-\infty}^{\infty} e^{ick(x-w_2)}e^{-k^2t}\left[\frac{1}{\gamma}\tilde{u}_{2x}(w_2,k^2)+ick\tilde{u}_2(w_2,k^2)\right]dk. \tag{38c}$$

Furthermore, the analyticity of the functions involved in the integral representation of the solutions $u_\ell(x,t)$ above, allows the replacement of the real axis $(-\infty,\infty)$ by other contours of integration in the complex plane. Indeed referring, for example, to the integral representation of $u_1(x,t)$ in (36), it can be easily observed that:

- the term $e^{ick(x-w_1)}$ is bounded and analytic for $\mathrm{Im}(k)\le 0$
- the term $e^{ick(x-a)}$ is bounded and analytic for $\mathrm{Im}(k)\ge 0$
- the term e^{-k^2t} is bounded and analytic for $\mathrm{Re}(k^2)\ge 0$.

Then, upon definition of the domains D, D^+ and D^- (see also Fig. 3) as

$$D=\{k\in\mathbb{C}:\mathrm{Re}\,k^2<0\}=\left\{k\in\mathbb{C}:\arg k\in\left\{\left(\frac{\pi}{4},\frac{3\pi}{4}\right)\cup\left(\frac{5\pi}{4},\frac{7\pi}{4}\right)\right\}\right\} \tag{39}$$

Please cite this article in press as: D. Mantzavinos et al., Fokas transform method for a brain tumor invasion model with heterogeneous diffusion in 1 + 1 dimensions, Applied Numerical Mathematics (2014), http://dx.doi.org/10.1016/j.apnum.2014.09.006

$$D^+ = \left\{k : \arg k \in \left(\frac{\pi}{4}, \frac{3\pi}{4}\right)\right\} = D \cap \mathbb{C}^+ \tag{40}$$

$$D^- = \left\{k : \arg k \in \left(\frac{5\pi}{4}, \frac{7\pi}{4}\right)\right\} = D \cap \mathbb{C}^- \tag{41}$$

we may equivalently express (see also [8]) the integral representations of $u_\ell(x,t)$ as

$$u_1(x,t) = \frac{c}{2\pi}\int_{-\infty}^{\infty} e^{ickx}e^{-k^2t}\widehat{f}_1(ck)dk \tag{42a}$$

$$-\frac{1}{2c\pi}\int_{\partial D^-} e^{ick(x-w_1)}e^{-k^2t}\left[\widetilde{u}_{1x}\left(w_1,k^2\right)+ick\widetilde{u}_1\left(w_1,k^2\right)\right]dk \tag{42b}$$

$$-\frac{1}{2\pi}\int_{\partial D^+} ike^{ick(x-a)}e^{-k^2t}\widetilde{u}_1\left(a,k^2\right)dk \tag{42c}$$

$$u_2(x,t) = \frac{1}{2\pi}\int_{-\infty}^{\infty} e^{ikx-k^2t}\hat{f}_2(k)dk \tag{43a}$$

$$-\frac{1}{2\pi}\int_{\partial D^-} e^{ik(x-w_2)}e^{-k^2t}\left[\tilde{u}_{2x}\left(w_2,k^2\right)+ik\tilde{u}_2\left(w_2,k^2\right)\right]dk \tag{43b}$$

$$-\frac{1}{2\pi}\int_{\partial D^+} e^{ik(x-w_1)}e^{-k^2t}\left[\gamma\tilde{u}_{1x}\left(w_1,k^2\right)+ik\tilde{u}_1\left(w_1,k^2\right)\right]dk \tag{43c}$$

$$u_3(x,t) = \frac{c}{2\pi}\int_{-\infty}^{\infty} e^{ickx-k^2t}\hat{f}_3(ck)dk \tag{44a}$$

$$-\frac{1}{2\pi}\int_{\partial D^-} e^{ick(x-b)}e^{-k^2t}ik\tilde{u}_3\left(b,k^2\right)dk \tag{44b}$$

$$-\frac{1}{2c\pi}\int_{\partial D^+} e^{ick(x-w_2)}e^{-k^2t}\left[\frac{1}{\gamma}\tilde{u}_{2x}\left(w_2,k^2\right)+ick\tilde{u}_2\left(w_2,k^2\right)\right]dk. \tag{44c}$$

To determine the quantities $\widetilde{u}_1(a,k^2)$, $\widetilde{u}_1(w_1,k^2)$, $\widetilde{u}_{1x}(w_1,k^2)$, $\tilde{u}_2(w_2,k^2)$, $\tilde{u}_{2x}(w_2,k^2)$, $\tilde{u}_3(b,k^2)$ we replace k by $-k$ in Eqs. (33)–(35) to obtain:

$$e^{k^2t}\widehat{u}_1(-ck,t) = \widehat{f}_1(-ck) + \gamma e^{ickw_1}\left[\widetilde{u}_{1x}\left(w_1,k^2\right) - ick\widetilde{u}_1\left(w_1,k^2\right)\right] + \gamma e^{icka}ick\widetilde{u}_1\left(a,k^2\right), \quad k\in\mathbb{C} \tag{45}$$

$$e^{k^2t}\widehat{u}_2(-k,t) = \widehat{f}_2(-k) + e^{ikw_2}\left[\widetilde{u}_{2x}\left(w_2,k^2\right) - ik\widetilde{u}_2\left(w_2,k^2\right)\right] - e^{ikw_1}\left[\gamma\widetilde{u}_{1x}\left(w_1,k^2\right) - ik\widetilde{u}_1\left(w_1,k^2\right)\right], \quad k\in\mathbb{C} \tag{46}$$

$$e^{k^2t}\widehat{u}_3(-ck,t) = \widehat{f}_3(-ck) - \gamma e^{ickb}ick\widetilde{u}_3\left(b,k^2\right) - \gamma e^{ickw_2}\left[\frac{1}{\gamma}\widetilde{u}_{2x}\left(w_2,k^2\right) - ick\widetilde{u}_2\left(w_2,k^2\right)\right], \quad k\in\mathbb{C}. \tag{47}$$

Eqs. (33), (45), (34), (46), (35), (47) define the linear system

$$G\tilde{\boldsymbol{u}} = \boldsymbol{f} \tag{48}$$

where

Please cite this article in press as: D. Mantzavinos et al., Fokas transform method for a brain tumor invasion model with heterogeneous diffusion in 1 + 1 dimensions, Applied Numerical Mathematics (2014), http://dx.doi.org/10.1016/j.apnum.2014.09.006

$$G=\begin{bmatrix} ick\gamma e^{-icka} & -\gamma icke^{-ickw_1} & -\gamma e^{-ickw_1} & & & & \\ -ick\gamma e^{icka} & \gamma icke^{ickw_1} & -\gamma e^{ickw_1} & & & & \\ & ike^{-ikw_1} & \gamma e^{-ikw_1} & -ike^{-ikw_2} & -e^{-ikw_2} & & \\ & -ike^{ikw_1} & e^{ikw_1}\gamma & ike^{ikw_2} & -e^{ikw_2} & & \\ & & & e^{-ickw_2}ick\gamma & e^{-ickw_2} & -ick\gamma e^{-ickb} & \\ & & & -e^{ickw_2}ick\gamma & e^{ickw_2} & ick\gamma e^{ickb} & \end{bmatrix} \tag{49}$$

$$\tilde{\boldsymbol{u}}=\begin{bmatrix} \widetilde{u}_1(a,k^2) \\ \widetilde{u}_1(w_1,k^2) \\ \widetilde{u}_{1x}(w_1,k^2) \\ \widetilde{u}_2(w_2,k^2) \\ \widetilde{u}_{2x}(w_2,k^2) \\ \widetilde{u}_3(b,k^2) \end{bmatrix}, \qquad \boldsymbol{f}=\begin{bmatrix} \widehat{f}_1(ck) \\ \widehat{f}_1(-ck) \\ \widehat{f}_2(k) \\ \widehat{f}_2(-k) \\ \widehat{f}_3(ck) \\ \widehat{f}_3(-ck) \end{bmatrix}. \tag{50}$$

Apparently, the solution of the above linear system determines the needed unknown quantities.

Remark 1. We point out that the Fourier transform terms $\widehat{u}_\ell(\pm ck,t)$ have been omitted from the system (48) as the contribution of $\frac{\widehat{u}_\ell(\pm ck,t)}{\det(G)}$ terms vanish (cf. [10]).

Remark 2. The presence of exponential terms, depending on k and at the same time on $-k$, in the system (48) above imposes the usage of appropriate normalization to avoid overflows. Division of each equation by its greatest in modulus coefficient suffices to resolve this problem.

3. Contours and properties of integration

Aiming to the development of efficient numerical integration rules, in this section we discuss appropriate contours of integration as well as we underline inherent properties of the integrals involved in relations (42)–(44).

3.1. Analytic expressions for integrals of Gaussian functions

Recalling the definitions (10) and (30) it becomes apparent that

$$f_\ell(x)=\begin{cases}\delta(x-\xi), & \xi\in\mathcal{R}_\ell\setminus\{l_\ell,r_\ell\}\\ 0, & \text{otherwise}\end{cases}, \quad \ell=1,2,3 \tag{51}$$

hence

$$\widehat{f}_\ell(\lambda k)=\begin{cases}e^{-i\lambda k\xi}, & \xi\in\mathcal{R}_\ell\setminus\{l_\ell,r_\ell\}\\ 0, & \text{otherwise}\end{cases} \tag{52}$$

and therefore the first integral term in (42)–(44)

$$\begin{aligned} u_{\ell a}(x,t) &:= \frac{\lambda}{2\pi}\int_{-\infty}^{\infty} e^{i\lambda kx}e^{-k^2t}\widehat{f}_\ell(\lambda k)dk \\ &= \begin{cases}\frac{\lambda}{2\sqrt{t\pi}}e^{-\frac{\lambda^2(\xi-x)^2}{4t}}, & \xi\in\mathcal{R}_\ell\setminus\{l_\ell,r_\ell\}\\ 0, & \text{otherwise}\end{cases} \end{aligned} \tag{53}$$

with $\lambda=c$ when $\ell=1,3$ and $\lambda=1$ when $\ell=2$.

Apparently, relation (59) is also being used to evaluate the right hand side vector $\boldsymbol{f}$, defined in (57), of the complex linear system in (55).

3.2. Integration contours

It is known (cf. [16,17]) that one approach to the numerical quadrature of integrals containing e^z is to apply the trapezoid rule on a suitable chosen contour. Hyperbolas, one class of such contours, are simple curves having asymptotic directions and are therefore a natural choice of integration path. To define the hyperbolas (see also [3,9]) we map the points θ on the real line to the points $\pm k(\theta)$ of the complex plane by using the analytic function:

$$k_\theta\equiv k(\theta):=i\sin(\beta-i\theta). \tag{54}$$

Evidently the $k(\theta)$ and $-k(\theta)$ curves replace the integration paths ∂D^+ and ∂D^- respectively (see Fig. 4).

Please cite this article in press as: D. Mantzavinos et al., Fokas transform method for a brain tumor invasion model with heterogeneous diffusion in $1+1$ dimensions, Applied Numerical Mathematics (2014), http://dx.doi.org/10.1016/j.apnum.2014.09.006

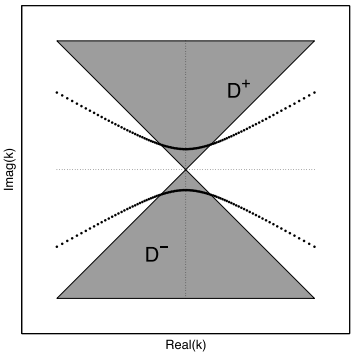

Fig. 4. The hyperbolas at $\beta = \pi/6$.

Furthermore, upon their substitution in (42)–(44), the integral representations of the solutions $u_\ell(x,t)$ take the form

$$u_\ell(x,t) = u_{\ell a}(x,t) + u_{\ell b}(x,t) + u_{\ell c}(x,t), \quad \ell = 1,2,3 \tag{55}$$

where $u_{\ell a}$ is as defined in (53), and

$$\begin{aligned}
u_{1b}(x,t) &= +\frac{1}{2c\pi}\int_{-\infty}^{\infty} e^{ick_\theta(w_1-x)}e^{-k_\theta^2 t}\left[\widetilde{u}_{1x}\left(w_1,k_\theta^2\right) - ick_\theta\widetilde{u}_1\left(w_1,k_\theta^2\right)\right]k'_\theta d\theta \\
u_{2b}(x,t) &= +\frac{1}{2\pi}\int_{-\infty}^{\infty} e^{ik_\theta(w_2-x)}e^{-k_\theta^2 t}\left[\widetilde{u}_{2x}\left(w_2,k_\theta^2\right) - ik_\theta\widetilde{u}_2\left(w_2,k_\theta^2\right)\right]k'_\theta d\theta \\
u_{3b}(x,t) &= -\frac{1}{2\pi}\int_{-\infty}^{\infty} e^{ick_\theta(b-x)}e^{-k_\theta^2 t}ik_\theta\widetilde{u}_3\left(b,k_\theta^2\right)k'_\theta d\theta \\
u_{1c}(x,t) &= -\frac{1}{2\pi}\int_{-\infty}^{\infty} ik_\theta e^{ick_\theta(x-a)}e^{-k_\theta^2 t}\widetilde{u}_1\left(a,k_\theta^2\right)k'_\theta d\theta \\
u_{2c}(x,t) &= -\frac{1}{2\pi}\int_{-\infty}^{\infty} e^{ik_\theta(x-w_1)}e^{-k_\theta^2 t}\left[\gamma\widetilde{u}_{1x}\left(w_1,k_\theta^2\right) + ik_\theta\widetilde{u}_1\left(w_1,k_\theta^2\right)\right]k'_\theta d\theta \\
u_{3c}(x,t) &= -\frac{1}{2c\pi}\int_{-\infty}^{\infty} e^{ick_\theta(x-w_2)}e^{-k_\theta^2 t}\left[\frac{1}{\gamma}\widetilde{u}_{2x}\left(w_2,k_\theta^2\right) + ick_\theta\widetilde{u}_2\left(w_2,k_\theta^2\right)\right]k'_\theta d\theta
\end{aligned} \tag{56}$$

with k'_θ to denotes the derivative of $k(\theta)$, namely

$$k'_\theta = \cos(\beta - i\theta). \tag{57}$$

3.3. Integrand algebraic properties

For the efficient evaluation of all the above integrals one has to take into consideration the following basic integrand algebraic properties:

- The real parts of all integrands are *even* functions of θ.
- The imaginary parts of all integrands are *odd* functions of θ.
- The integrands are decaying functions of θ.

The proof of the first two properties follows after a few algebraic manipulations (cf. [8]) while the third one is a direct consequence of the selected integration paths. Said properties are further demonstrated through Figs. 5, 6 and 7 for the integrals u_{1b} and u_{1c}. Application of the above properties directly implies that

Please cite this article in press as: D. Mantzavinos et al., Fokas transform method for a brain tumor invasion model with heterogeneous diffusion in 1 + 1 dimensions, Applied Numerical Mathematics (2014), http://dx.doi.org/10.1016/j.apnum.2014.09.006

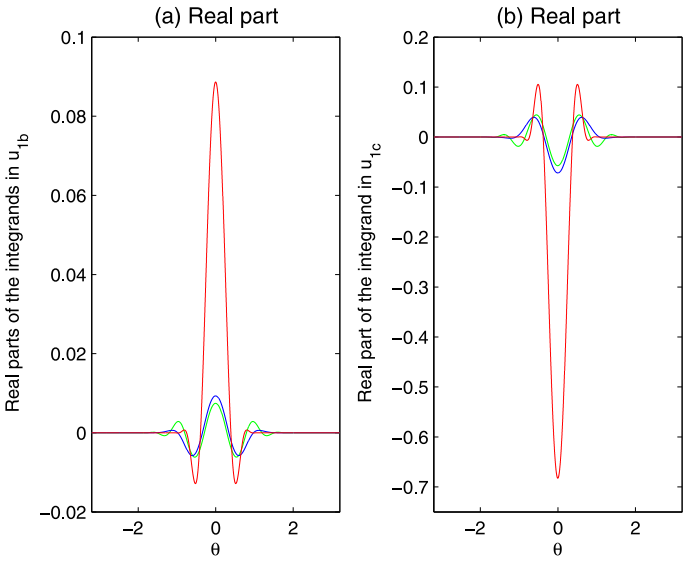

Fig. 5. Real parts of the integrands in (*a*) u_{1b} and (*b*) u_{1c} integrals for $x=-\pi$ and $t=0.1$ (green), $t=1$ (blue), $t=10$ (red). (For interpretation of the references to color in this figure legend, the reader is referred to the web version of this article.)

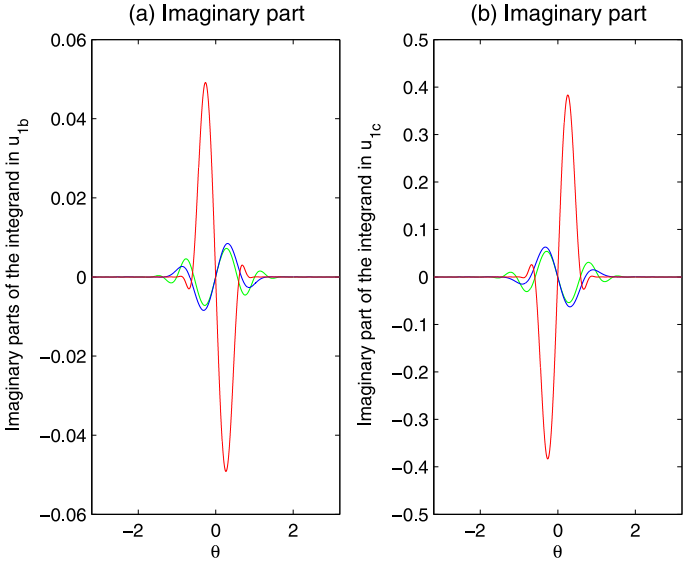

Fig. 6. Imaginary parts of the integrands in (*a*) u_{1b} and (*b*) u_{1c} integrals for $x=-\pi$ and $t=0.1$ (green), $t=1$ (blue), $t=10$ (red). (For interpretation of the references to color in this figure legend, the reader is referred to the web version of this article.)

$$\int_{-\infty}^{\infty} U(\theta)d\theta = 2\int_{0}^{\infty} \mathrm{Re}\big(U(\theta)\big)d\theta \approx 2\int_{0}^{R} \mathrm{Re}\big(U(\theta)\big)d\theta,$$

where $U(\theta)$ denotes any one of the integrands involved in (56) and R is a relatively *small* real number. For a good estimate of R one may ask the dominant exponential term $e^{-k_\theta^2 t}$, common in all integrals, to satisfy

$$\left|e^{-k_\theta^2 t}\right| \leq 10^{-M} \quad \text{for all } \theta \geq R \equiv R(t;M)$$

for sufficiently large M, hence

$$R = \frac{1}{2}\ln\frac{4t+8M\ln 10}{t}. \tag{58}$$

Please cite this article in press as: D. Mantzavinos et al., Fokas transform method for a brain tumor invasion model with heterogeneous diffusion in 1 + 1 dimensions, Applied Numerical Mathematics (2014), http://dx.doi.org/10.1016/j.apnum.2014.09.006

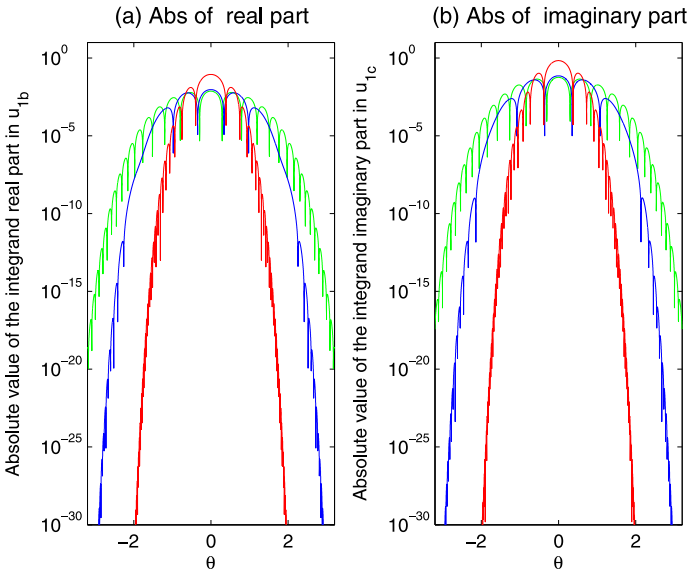

Fig. 7. Absolute value of the integrand real part (logarithmic scale) of (*a*) u_{1b} and (*b*) u_{1c} integrals for $x=-\pi$ and $t=0.1$ (green), $t=1$ (blue), $t=10$ (red). The corresponding values of R from (58) are given respectively by $R=4.31,\ 3.16,\ 2.04$ for $M=30$. (For interpretation of the references to color in this figure legend, the reader is referred to the web version of this article.)

4. Numerical evaluation

Recalling relations (7)–(9) and (14), which completely define the model problem at hand, and referring to Fig. 2, the model data used in this section are given by:

$$a=-5, \qquad w_1=-1, \qquad w_2=1, \qquad b=5,$$
$$u(x,0)=\delta(x+3) \quad \text{and} \quad u(x,0)=\delta(x+4)+\delta(x-2). \tag{59}$$

The dimensionless diffusion coefficient in grey matter γ is taking the value $\gamma=0.2$, namely $D_w=5D_g$, characterizing high grade gliomas (see Table 1). For comparison purposes, we have also included the same experiments for $\gamma=0.5$ (see Fig. 8).

In all numerical simulations the time t evolves up to $t_{\max}=4$, which corresponds to approximately 1 year of real time (11 months 3 days and 8 hours, to be exact), suggested by medical data for high grade gliomas (see Table 1). In Table 2, we show the relation between dimensionless are real time for certain characteristic values. Furthermore the hyperbolas, adopted as numerical contours, use $\beta=\pi/6$ as in [9], while no significant difference is noticed if we choose other qualified (less than $\pi/4$) values of β, say $\beta=\pi/8$ used in [3].

For the quadrature of the integrals in (56) the hyperbolic contours are combined with a simple 64-point trapezoid rule (cf. [16,17]) to achieve a fast decaying rate of convergence.

Implementing the above described procedure, the time evolution of the tumor cell density

$$c(x,t)=e^t u(x,t)$$

can be numerically observed, as we have done in Fig. 8 for $0.2\le t\le 4$ with time step $dt=0.2$. In Fig. 8, different line curves represent the tumor cell density at different time levels. The diffusivity factor γ has been set to $\gamma=0.5$ in Figs. 8a and 8c, while in Figs. 8b and 8d has been set to $\gamma=0.2$. The initial tumor sell density has been considered to be $u(x,0)=\delta(x+3)$ in Figs. 8a and 8b, and $u(x,0)=\delta(x+4)+\delta(x-2)$ in Figs. 8c and 8d.

The computational time needed to compute the numerical approximation of $u(x,t)$ at a certain point $(x,t)=(\bar{x},\bar{t})$, is essentially the computational time needed to construct and solve the linear system in (48) for each one of the quadrature points. Using Matlab, a 64-point trapezoid rule and taking into account the integral symmetries, the approximation of $u(\bar{x},\bar{t})$ on a nowadays PC takes a few milliseconds for the solution of the linear systems involved, and tenths of a millisecond for the completion of the numerical integration. It is worthwhile to point out that the linear system in (48) does not depend on the variables x and t, depending only on the variable $k=k(\theta)$. Therefore, for fixed $t=\bar{t}$, hence same $R=R(\bar{t})$ and thus same quadrature points for all integrals, the computational time needed to compute the numerical approximation of $u(x,t)$ at M points $(\bar{x}_j,\bar{t})$, $j=1,\ldots,M$, is almost equal to the time needed for the numerical approximation of $u(x,t)$ at one point since we can construct and solve the linear systems involved once and use in the sequel their solution for all integrals at all points.

Please cite this article in press as: D. Mantzavinos et al., Fokas transform method for a brain tumor invasion model with heterogeneous diffusion in 1 + 1 dimensions, Applied Numerical Mathematics (2014), http://dx.doi.org/10.1016/j.apnum.2014.09.006

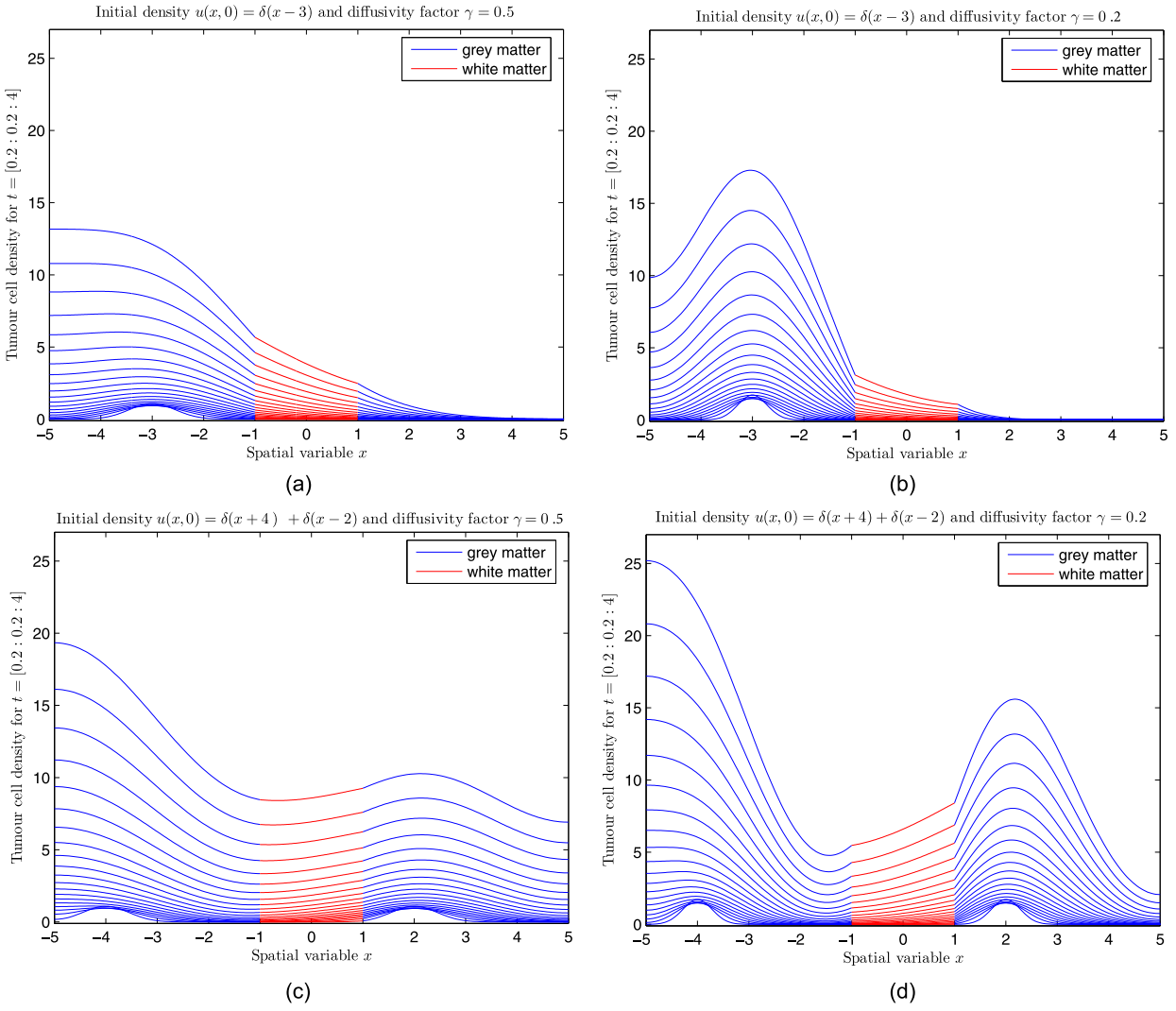

Fig. 8. Time evolution of the tumor cell density $c(x,t)$ for $t = 0.2 : 0.2 : 4$.

Table 2
Characteristic values of dimensionless are real time for high grade tumors.

Dimensionless time	Real time
$t = 0.01$	20 hours
$t = 0.1$	$\approx$ 8 days
$t = 1$	$\approx$ 3 months
$t = 4$	$\approx$ 1 year
$t = 10$	$\approx$ 2 years

The convergence rate of the numerical integration procedure is basically affected by the choice of the parameter R, which determines the integration limits, and the number of the quadrature points N. To explore the dependence on the parameter R we make use of the relative error E_R, defined by:

$$E_R := \frac{\|U_{R_i} - U_{R_{i+1}}\|_\infty}{\|U_{R_{i+1}}\|_\infty}, \tag{60}$$

where U_{R_i} denotes the vector of numerical approximations $\hat{u}(\bar{x}_j, \bar{t}; R_i)$, $j = 1, \ldots, M$ to the solution $u(x,t)$ produced by using $[-R_i, R_i]$ as integration limits in all integrals. Referring to the model problem described in Fig. 8a and keeping N

Please cite this article in press as: D. Mantzavinos et al., Fokas transform method for a brain tumor invasion model with heterogeneous diffusion in $1+1$ dimensions, Applied Numerical Mathematics (2014), http://dx.doi.org/10.1016/j.apnum.2014.09.006

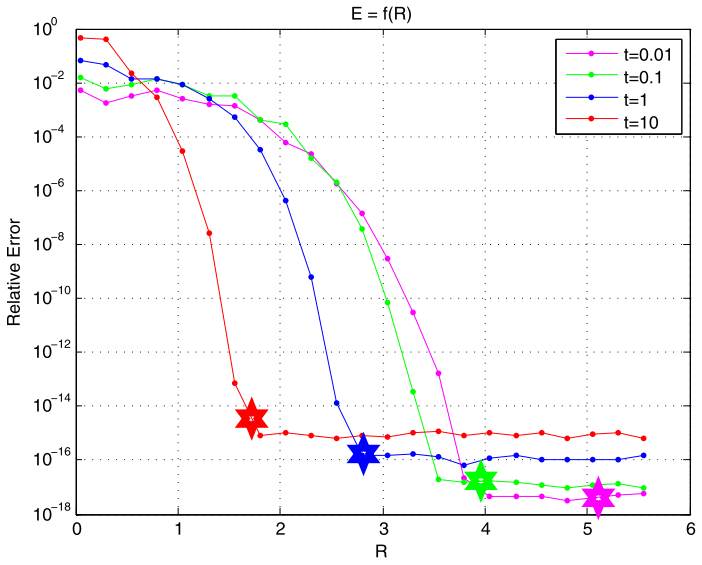

Fig. 9. The relative error E_R for different values of time (t).

fixed at a sufficiently large $(N \geq 64)$ value, the relative error E_R is depicted in Fig. 9. Observe that there is an optimal value R_{opt} such that the relative error E_R remains practically the same for all $R \geq R_{opt}$. The value $R = R_s$, obtained by using relation (58) and shown schematically by a *"star"* in Fig. 9, is clearly an effective approximation to R_{opt}.

To explore now the dependence on the number of the quadrature points N, we define the relative error E_N as:

$$E_N := \frac{\|U_{N_i} - U_{N_{i+1}}\|_\infty}{\|U_{N_{i+1}}\|_\infty} \tag{61}$$

where U_{N_i} denotes the vector of numerical approximations $\hat{u}(\bar{x}_j, \bar{t}; N_i)$, $j = 1, \ldots, M$ to the solution $u(x,t)$ produced by using N_i quadrature points with the trapezoid rule used for the numerical evaluation of all integrals. In Fig. 10 we observe the rapidly decaying convergence rate when $R = R_s$, the value obtained by using relation (58). Similar behavior is observed for all values of R in the neighborhood of R_{opt}. In these cases the error drops exponentially reaching 10^{-14} for $N \geq 64$. To the contrary, for $R < R_{opt}$ the convergence is slow. We remark that in [3] an adaptive trapezoid rule was adopted and implemented through known computational environments to overcome the need of increased quadrature points around zero $(0, t)$. The use, however, of adaptive procedures in our implementation is not a central issue as the computational cost in multi-domain environments is basically attributed to the solution of the involved linear system.

5. Conclusions

In this work we implemented effectively the Fokas transform method in a multi-region, multi-physics problem simulating brain tumor growth in heterogeneous environments (white–grey matter).

To overcome the singularities at interface points, Fokas integral representations of the solution in different regions are also coupled by a linear system, for the unknown quantities on the interface points, derived by making use of the global relationships evaluated not only at k but at $-k$ as well.

For the numerical evaluation of the integrals involved, taking into consideration the fast decaying properties of the integrands, we adopted hyperbolic contours and reduced the limits of integration from $(-\infty, \infty)$ to $(-R_{opt}, R_{opt})$, where R_{opt} is estimated in (58), to achieve exponentially decaying rate of convergence for a simple trapezoid quadrature rule. In this way, the computational cost of the whole numerical procedure is mainly attributed to the solution of the involved linear system.

Acknowledgement

The present research work has been co-financed by the European Union (European Social Fund – ESF) and Greek national funds through the Operational Program "Education and Lifelong Learning" of the National Strategic Reference Framework (NSRF) – Research Funding Program: THALIS. Investing in knowledge society through the European Social Fund.

Please cite this article in press as: D. Mantzavinos et al., Fokas transform method for a brain tumor invasion model with heterogeneous diffusion in $1+1$ dimensions, Applied Numerical Mathematics (2014), http://dx.doi.org/10.1016/j.apnum.2014.09.006

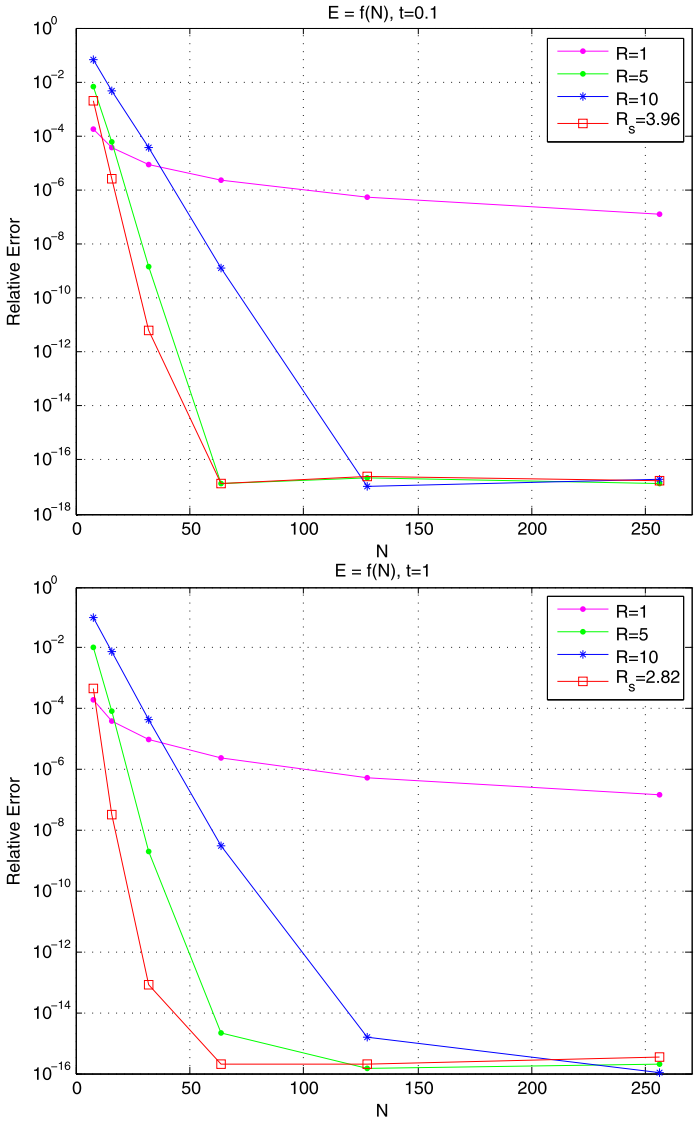

Fig. 10. The relative error E_N for $t = 0.1, 1$ and different values of R.

References

[1] P. Burgess, P. Kulesa, J. Murray, E. Alvord Jr., The interaction of growth rates and diffusion coefficients in a three-dimensional mathematical model of gliomas, J. Neuropathol. Exp. Neurol. 56 (1997) 704–713.
[2] G. Cruywagen, D. Woodward, P. Tracqui, G. Bartoo, J. Murray, E. Alvord, The modeling of diffusive tumours, J. Biol. Syst. 3 (1995) 937–945.
[3] N. Flyer, A.S. Fokas, A hybrid analytical–numerical method for solving evolution partial differential equations I. The half-line, Proc. R. Soc. A 464 (2008) 1823–1849.
[4] A.S. Fokas, A unified transform method for solving linear and certain nonlinear PDEs, Proc. R. Soc. Lond. Ser. A, Math. Phys. Sci. 453 (1997) 1411–1443.
[5] A.S. Fokas, A new transform method for evolution partial differential equations, IMA J. Appl. Math. 67 (2002) 559–590.
[6] A.S. Fokas, N. Flyer, S.A. Smitheman, E.A. Spence, A semi-analytical numerical method for solving evolution and elliptic partial differential equations, J. Comput. Appl. Math. 227 (2009) 59–74.
[7] J. Murray, Mathematical Biology, 3rd ed., Springer-Verlag, 2002.
[8] M. Papadomanolaki, The collocation method for parabolic differential equations with discontinuous diffusion coefficient: in the direction of brain tumour, Ph.D. thesis, Technical University of Crete, 2012.
[9] T.S. Papatheodorou, A.N. Kandili, Novel numerical techniques based on Fokas transforms, for the solution of initial boundary value problems, J. Comput. Appl. Math. 227 (2009) 75–82.
[10] D.A. Smith, Well-posed two-point initial-boundary value problems with arbitrary boundary conditions, Math. Proc. Camb. Philos. Soc. 152 (2012) 473–496.
[11] K. Swanson, Mathematical modeling of the growth and control of tumors, Ph.D. thesis, University of Washington, 1999.
[12] K. Swanson, Virtual and real brain tumors: using mathematical modeling to quantify glioma growth and invasion, J. Neurol. Sci. 216 (2003) 1–10.
[13] K. Swanson, E. Alvord Jr., J. Murray, A quantitative model for differential motility of gliomas in grey and white matter, Cell Prolif. 33 (2000) 317–329.

Please cite this article in press as: D. Mantzavinos et al., Fokas transform method for a brain tumor invasion model with heterogeneous diffusion in 1 + 1 dimensions, Applied Numerical Mathematics (2014), http://dx.doi.org/10.1016/j.apnum.2014.09.006

[14] K. Swanson, E. Alvord Jr., J. Murray, Virtual brain tumours (gliomas) enhance the reality of medical imaging and highlight inadequacies of current therapy, Br. J. Cancer 86 (2002) 14–18.
[15] P. Tracqui, G. Cruywagen, D. Woodward, G.T. Bartoo, J. Murray, E. Alvord, A mathematical model of glioma growth: the effect of chemotherapy on spatio-temporal growth, Cell Prolif. 28 (1995) 17–31.
[16] L.N. Trefethen, J.A.C. Weideman, T. Schmelzer, Talbot quadratures and rational approximations, BIT Numer. Math. 46 (2006) 653–670.
[17] J.A.C. Weideman, L.N. Trefethen, Parabolic and hyperbolic contours for computing the Bromwich integral, Math. Comput. 76 (2007) 1341–1356.
[18] D. Woodward, J. Cook, P. Tracqui, G. Cruywagen, J. Murray, E. Alvord Jr., A mathematical model of glioma growth: the effect of extent of surgical resection, Cell Prolif. 29 (1996) 269–288.

Please cite this article in press as: D. Mantzavinos et al., Fokas transform method for a brain tumor invasion model with heterogeneous diffusion in $1+1$ dimensions, Applied Numerical Mathematics (2014), http://dx.doi.org/10.1016/j.apnum.2014.09.006